A practical phosphorus-based anode material for high-energy lithium-ion batteries

Rachid Amine [a,b ‡], Amine Daali [c,d ‡], Xinwei Zhou [e,f ‡], Xiang Liu [c], Yuzi Liu [e], Yang Ren [g], Xiaoyi Zhang [g], Likun Zhu [f*], Said Al-Hallaj [a], Zonghai Chen [c], Gui-Liang Xu [c*], and Khalil Amine [c,h,*]

[a] *Department of Chemical Engineering, University of Illinois at Chicago, Chicago, Illinois 60607, USA*

[b] *Materials Science Division, Argonne National Laboratory, Lemont, IL 60439, USA*

[c] *Chemical Sciences and Engineering Division, Argonne National Laboratory, Lemont, IL 60439, USA*

[d] *University of Wisconsin-Milwaukee, 3200 North Cramer Street, Milwaukee, WI 53211, USA*

[e] *Center for Nanoscale Materials, Argonne National Laboratory, Lemont, IL 60439, USA*

[f] *Department of Mechanical and Energy Engineering, Indiana University - Purdue University Indianapolis, Indianapolis, IN 46202, USA*

[g] *X-ray Science Division, Argonne National Laboratory, Lemont, IL 60439, USA*

[h] *Materials Science and Engineering, Stanford University, Stanford, CA 94305, USA*

‡ These authors contributed equally.

*Corresponding author emails: amine@anl.gov (Khalil Amine), likzhu@iupui.edu (Likun Zhu) and xug@anl.gov (Gui-Liang Xu)

Abstract

State-of-the-art lithium-ion batteries cannot satisfy the increasing energy demand worldwide because of the low specific capacity of the graphite anode. Silicon and phosphorus both show much higher specific capacity; however, their practical use is significantly hindered by their large volume changes during charge/discharge. Although significant efforts have been made to improve their cycle life, the initial coulombic

This is the author's manuscript of the article published in final edited form as:

Amine, R., Daali, A., Zhou, X., Liu, X., Liu, Y., Ren, Y., Zhang, X., Zhu, L., Al-Hallaj, S., Chen, Z., Xu, G.-L., & Amine, K. (2020). A practical phosphorus-based anode material for high-energy lithium-ion batteries. Nano Energy, 74, 104849. https://doi.org/10.1016/j.nanoen.2020.104849

efficiencies of the reported Si-based and P-based anodes are still unsatisfactory (<90%). Here, by using a scalable high-energy ball milling approach, we report a practical hierarchical micro/nanostructured P-based anode material for high-energy lithium-ion batteries, which possesses a high initial coulombic efficiency of 91% and high specific capacity of ~ 2500 mAh g^{-1} together with long cycle life and fast charging capability. In situ high-energy X-ray diffraction and in situ single-particle charging/discharging were used to understand its superior lithium storage performance. Moreover, proof-of-concept full-cell lithium-ion batteries using such an anode and a $LiNi_{0.6}Co_{0.2}Mn_{0.2}O_2$ cathode were assembled to show their practical use. The findings presented here can serve as a good guideline for the future design of high-performance anode materials for lithium-ion batteries.

Keywords: Anode materials; lithium-ion batteries; high initial coulombic efficiency, phosphorus, full cell

Introduction

The increased energy demands of portable electronics and electric vehicles have significantly boosted the development of high-energy lithium-ion batteries (LIBs). An effective approach to increase the energy density of LIBs is to use high-capacity anode materials. Graphite, the state-of-the-art anode material, has a theoretical specific capacity of only 372 mAh g^{-1}, which cannot meet the requirements for increasing energy density and power density despite these anodes' long-term cycle stability and high initial coulombic efficiency (ICE)[1].

As an alternative, significant attention has been paid to silicon, which has an

extremely high theoretical gravimetric capacity of ~ 4200 mAh g^{-1}[2]. However, Si undergoes a huge volume expansion (>300%) during lithiation, leading to severe capacity degradation due to the pulverization and electrical isolation of Si particles upon cycling[3]. In addition, the *c*-$Li_{15}Si_4$ phase formed during deep lithiation of Si is rather reactive with the non-aqueous electrolytes, possible causing depletion of electrolytes and further capacity fading[4]. These parasitic reactions are aggravated upon pulverization of Si due to increased exposed surface area. A common practice to tackle these issues is to fabricate nanometer-sized Si materials such as nanowires[5] and porous Si[6], or integrate Si with various types of carbon matrix such as graphene[7] and graphite[8]. However, the use of nanometer-sized Si would significantly reduce the volumetric energy density because of its low tap density. More importantly, both nanometer-sized Si and Si/C composites suffer from inferior ICE (< 80%), which is a critical parameter for their practical application[9]. Most of the reported excellent cycle performance of Si anodes is based on the evaluation of half-cells, in which excess lithium is used as a reference electrode and thus compensates for the lithium loss caused by Si. However, in practical LIBs, as the limited amount of Li from the cathode host is consumed by Si, both the cathode and the Si anode will be degraded, eventually causing capacity fade in the cell [10]. Thus, the development of a practical anode material with high ICE (>90%), high capacity (>1000 mAh g^{-1}), and long cycle life for high-energy LIBs remains a huge challenge.

Besides graphite and Si, phosphorus, in particular black phosphorus (BP) and red phosphorus (RP), have attracted extensive attention as anodes for lithium-, sodium- and

potassium-ion batteries[11-13]. They have a moderate working potential of 0.9 and 0.45 V during charge and discharge, respectively. Moreover, as a result of a reversible alloying with Li to form Li_3P, both BP and RP have a high theoretical specific capacity of 2596 mAh g^{-1}; however, this process is accompanied by a large volume change (~ 300%) during lithiation[14, 15]. A transfer of knowledge about the mitigation of volume changes from the Si anode to the P anode has helped researchers to design and fabricate advanced P anode materials with stable cycle life. However, none of the reported P anodes, such as P-graphene[16-20], P@CNTs[21-23], hollow P nanospheres[15], P-porous carbon[12, 24], and iodine-doped RP[25] with a carbon coating [26], has achieved an ICE of over 90%.

Herein, we have reported a practical anode material for high-energy LIBs, consisting of a black phosphorus/Ketjenblack-MWCNTs (BPC) composite with 70 wt.% BP loading, fabricated through a scalable high-energy ball milling approach. In operando high-energy X-ray diffraction (HEXRD) during charge/discharge showed that this BPC anode demonstrates a highly reversible phase transformation during lithiation/de-lithiation. In situ single-particle charge/discharge experiments using focused ion beam scanning electron microscopy (FIB-SEM) clearly showed that the volume changes of the BPC anode during cycling are also well accommodated. As a result, the BPC anode demonstrates a high ICE of ~91% and a very high specific capacity of 2512.4 mAh g^{-1}, together with superior cycle stability (> 2000 mAh g^{-1}@100^{th} cycle) and excellent rate capability (~ 1600 mAh g^{-1}@6.24 A g^{-1}). Finally, the electrochemical performance of a full cell using the BPC anode and a commercial

$LiNi_{0.6}Co_{0.2}Mn_{0.2}O_2$ (NCM622) cathode was evaluated, indicating the feasibility of the BPC anode in practical LIBs.

Experimental Section

Materials synthesis

Synthesis of the BPC composite for use as the anode of sodium-ion batteries was previously reported in our work[13]. Red phosphorus/Ketjenblack-MWCNTs composite with 70% RP loading was synthesized in the present work using a similar procedure but replacing BP with RP.

Electrochemical measurement

The electrodes were prepared by spreading a mixture of 70 wt.% active material, 20 wt.% carbon black, and 10 wt.% carboxymethyl cellulose sodium salt (2 wt.%) onto a copper foil current collector. The as-prepared electrode was dried at 80°C in a vacuum oven for 24 h. The loading of active P in the electrode was controlled at about 1.0–1.5 mg cm^{-2}. The electrochemical performance of the P-based electrodes was characterized by assembling them into coin cells (type CR2032) in an argon-filled glove box under conditions such that the moisture and oxygen contents were both below 1.0 ppm. The anode was separated from the lithium counter-electrode by a separator (Celgard 2325). The electrolytes were carbonated electrolytes (GEN II), which are composed of $LiPF_6$ (1.2M) dissolved in ethylene carbonate and ethyl methyl carbonate (3:7 vol.%), with 10 wt.% fluoroethylene carbonate as additive. The cells were charged and discharged in a MACCOR system with a voltage range of 0.02–2.0 V (*vs.* Li/Li^+). Cyclic voltammograms were recorded on a Solartron Analytical 1470 System between 0.01

and 2.0 V (*vs.* Li/Li^+) at 0.1 mV s^{-1}. Electrochemical impedance spectroscopy of the Li/BPC coin cells before and after cycling was performed with a Solartron Analytical 1470 System in a frequency range of 100 kHz to 0.1 Hz.

Full-cell investigation

To investigate the potential of BPC in a Li metal-free battery, we carried out a full-cell test by coupling a BPC anode and NCM622 cathode. The NCM622 cathode was provided by an industry partner. The NCM622 electrodes were prepared by spreading a mixture of 90 wt.% active material, 5 wt.% C45, and 5 wt.% PVDF (8 wt.% in NMP) onto an aluminum foil current collector. The as-prepared electrodes were then dried at 100°C in a vacuum oven for 12 h. The loading density of NCM622 in the electrodes was controlled at 9 mg cm^{-2}. The BPC/NCM622 full cell was then tested within 1.3–4.2 V with a negative/positive ratio of around 1.1/1. In a typical cell, the active mass of the NCM622 cathode is 14.08 mg, and that of the BPC anode is set at 1.16 mg. The specific capacities and current densities for the BPC/NCM622 full cell were calculated on the basis of the active mass of the NCM622 cathode.

In situ synchrotron HEXRD

The in situ synchrotron HEXRD measurement was carried out at Beamline 11-ID-D of the Advanced Photon Source at Argonne National Laboratory. The X-ray wavelength was 0.799898 Å. In situ synchrotron HEXRD patterns were collected with custom-designed coin cells cycled with a MACCOR cycler at C/10 (1 C= 2600 mA g^{-1}) between 0.02 and 2.0 V. During the charging and discharging, the XRD patterns were collected for 1 min at 10-min intervals, using a Perkin-Elmer 2D X-ray detector. 2D images were

converted into a 1D plot of 2θ versus intensity by using the FIT2D program calibrated against a CeO_2 standard.

In situ single-particle charge/discharge inside a scanning electron microscope

The setup of the in situ experiments with a single BPC particle during charge/discharge can be found in our previous work [27]. Typically, to build a single-particle battery cell, a BPC particle attached to a tungsten probe by ion-beam carbon deposition served as the positive electrode. Lithium metal was placed on top of the scanning electron microscope stub to serve as the negative electrode. One drop of ionic liquid electrolyte (ILE) was placed on top of the Li metal. The single-particle battery cycling was controlled by a Keithley 6430 sub-femtoamp remote SourceMeter from Tektronix. The particle was immersed in the ILE drop during cycling and lifted out for imaging in different states of charge and discharge. The ILE was made by dissolving the Li salt, lithium bis (trifluoromethylsul-fonyl) imide (LiTFSI), in a solvent of 1-butyl-1-methylpyrrolidinium bis (trifluoromethylsulfonyl) imide (P_{14}TFSI). The particle was immersed in the ILE drop during cycling and lifted out for imaging at different states of charge and discharge. The voltage window was between 0.02 and 2.0 V. To visualize the microstructural change of the particle, the imaging area was polished by a focused ion beam to remove the ILE from the surface.

Results and discussion

The structure of the BPC composites has been characterized in our previous work[13]; they are composed of micrometer-sized secondary particles consisting of nanometer-sized (5- to 10-nm). primary particles. Such hierarchical

micro/nanostructures could not only increase the tap density of the material, but also could well accommodate the volume changes during charge/discharge. When the BPC composite was used as the anode in sodium-ion batteries, it demonstrated excellent sodium storage performance in terms of specific capacity and cycle stability[13]. In the present work, we further evaluate its feasibility as the anode for practical high-energy LIBs.

Cyclic voltammetry (CV) was used to understand the BPC anode's lithiation/de-lithiation behavior during charge/discharge. Figure 1 shows the first four cycles of CV profiles of the BPC anode at a scan rate of 0.1 mV s^{-1}. In the first cathodic scan, there was a large reduction peak starting at ~ 1.0 V and centered at ~ 0.4 V, which corresponds to the stepwise lithiation of phosphorus. This peak shifted to a more positive potential and was split into three distinct peaks at 1.26 V, 0.66 V, and 0.5 V in the subsequent cycles; this behavior can be attributed to the formation of different Li_xP phases (x=1–3)[18]. Such peak shift during CV test was also reported in other P-based anode materials for LIBs and sodium-ion batteries[13, 18, 23, 25]. This is because CV is potential sweep rate (i.e., mV s^{-1}) controlled, rather than constant current controlled. This forced change in the potential, is independent on the state of charge of the electrode, can increase the current beyond the kinetic limit of the cell, resulting in some capacity from being accessed and hence the activation process observed in the CV. During the anodic scan, there was a strong peak centered at 1.24 V with two weak peaks at 1.07 V and 1.57 V, corresponding to the de-lithiation of the Li_xP phase[18]. Moreover, it can be clearly seen that the CV curves after the first cycle were highly overlapped,

indicating that the BPC has excellent lithiation/de-lithiation reversibility.

To confirm the highly reversible lithiation/de-lithiation of the BPC anode, we further conducted in operando HEXRD using custom-designed coin cells to track the phase transformation of the BPC anode during charge/discharge at 0.1 C (1 C=2600 mA g^{-1}). As shown in Figure 2a, the charge/discharge curve of the in situ coin cell can deliver a high and reversible capacity of ~ 2500 mAh g^{-1}, indicating that the lithiation/de-lithiation process in the BPC anode was not affected by using such a cell design. The HEXRD pattern of the pristine BPC anode (Figure 2b) exhibited only two weak and broad peaks at ~ 11°, confirming the amorphous structure of the BPC anode caused by the breakdown of particle size after high-energy ball milling. During lithiation, the BPC anode remained amorphous in structure until the cell was discharged to 0.48 V. Multiple peaks centered at around 10°, 11.3°, 17.5°, 20.2°, 25° and 27° can be clearly seen, and are very likely to be due to the formation of crystalline Li_xP (x=1–3). When the cell was further discharged to 0.02 V, the intensities of these peaks increased as a result of the continuous lithiation between Li and the BPC. Upon de-lithiation, these peaks gradually disappeared as a result of the de-alloying of the Li_xP phase. At the end of the charge process, the BPC anode has completely returned to an amorphous structure, strongly confirming that the lithiation/de-lithiation of the BPC anode is highly reversible.

The HEXRD results serve as a good proof of the excellent structural stability of the BPC anode during charge/discharge. To confirm this stability, we further conducted in situ FIB-SEM to directly visualize the morphological changes of single BPC particles

during charge/discharge. This setup has been successfully used in our previous work to examine the structural changes in single-particle anode materials, e.g., Sn[27] and Ge[28], during charge/discharge. A single BPC particle was charged/discharged at 0.2 C (~100 pA) for the first cycle, 0.6 C (~300 pA) for the second cycle, and then 1.2 C (~ 600 pA) for the third to ninth cycles. Figure 3a shows the voltage profile of a single BPC particle charge/discharge at 0.2 C, which exhibited similar charge/discharge capacity to the coin-cell result. Thus, the morphological changes measured by using this approach can reflect the practical volume changes during lithiation/de-lithiation of the BPC anode. Figures 3b–3h show SEM images of the BPC anode at different stages of charge/discharge and different cycles. As shown, the BPC particle expanded during discharge and contracted during charge. However, no obvious particle pulverization can be observed during successive cycling (total of 9 cycles) and even at high rates (up to 1.2 C). Figure 3j gives an estimation of the length variation of the BPC particles in two directions. It can be seen that although the BPC anode cannot completely return to the length of the pristine state, the length values are relatively stable during cycling, indicating that the volume changes of the BPC anode have been well accommodated. A close examination of the cross-section of the BPC particle depicted in Figures 3j–3l clearly shows that the hierarchical micro/nanostructures of the BPC anode are well maintained during charge/discharge.

Thus, the in situ HEXRD and in situ FIB-SEM experiments have clearly confirmed that the BPC anode demonstrates excellent mechanical and structural stability during lithiation/de-lithiation, which could thus effectively suppress the

parasitic reactions with the electrolytes during long-term and high-temperature cycling and thus lead to superior lithium storage performance. The electrochemical performance of the BPC anodes was evaluated by assembling them into Li/BPC half-cells and charging/discharging within the range of 0.02–2.0 V. Figure 4a shows the first, second, and 100th charge/discharge voltage profiles of the BPC anode during cycling at 0.2 C. As shown, unlike the first charge/discharge curve of other P-based anode materials that usually exhibit a slope plateau above 1.0 V because of solid-electrolyte interphase (SEI) formation during discharge[22, 25], the BPC anode showed only negligible capacity when the cell was discharged from open-circuit voltage to 1.0 V. This finding indicates that the irreversible decomposition of the electrolytes to form SEI has been significantly suppressed with the BPC anode. Below 1.0 V, the BPC anode exhibited a long discharge plateau at ~ 0.75 V, which is related to the lithiation of the BPC anode. The initial discharge specific capacity is measured to be 2775.2 mAh g^{-1}, which is only slightly higher than the theoretical capacity of P anode. This strongly confirms the suppressed decomposition of electrolytes in our BPC anode during charge/discharge. During charging, the BPC anode displayed a long charge plateau of ~1.1 V and delivered a reversible capacity as high as 2512.4 mAh g^{-1}, leading to a high utilization of 96.8%. This behavior also resulted in a high ICE of ~ 91%, which has surpassed many reported results, as shown in Figure 4b. Such a significant improvement in the ICE of the BPC anode is mainly attributed to its unique structural design, which can well accommodate the huge volume changes during lithiation/de-lithiation and remarkably reduce the irreversible electrolyte decomposition. Note that

we believe the initial irreversible capacity loss (~10%) of the BPC anode should come mainly from the irreversible insertion of Li^+ into the Ketjenblack/MWCNTs matrix. As shown in Figure 4c, the pure Ketjenblack/MWCNTs matrix suffers from a large irreversible capacity loss during the first cycle. Thus, decreasing the amount of Ketjenblack/MWCNTs in the BPC composite may further improve the ICE. However, there is obviously a trade-off between cycle stability and ICE. In our work, the optimal loading of BP in the BPC composite is limited to 70 wt.%. Figure 4d shows the cycle performance of the BPC anode at 0.2 C; the BPC anode was able to maintain a high reversible capacity of > 2000 mAh g^{-1} after 100 cycles, indicating excellent cycle stability. Given the high loading of BP (70 wt.%) in the BPC composite, the overall capacity of the composite is higher than 1400 mAh $g^{-1}_{composite}$. The tap density of the BPC composite was measured to be ~ 0.8 cc g^{-1}, resulting in a high volumetric specific capacity of > 1120 mAh $cc^{-1}_{composite}$. The coulombic efficiency of the BPC anode increases to almost 100% after the first cycle, showing high lithiation/de-lithiation reversibility (Figure 4e). To better understand the reason for the improved cycle stability of the BPC anode, we conducted electrochemical impedance spectroscopy, as shown in Figure 4f. After 100 cycles of charge/discharge, the surface-film thickness and charge-transfer resistance of the cell were both very small, indicating that there is no significant decomposition of the electrolytes to form thicker and thicker SEI, and the electrical contact between the BPC and the current collector was also well maintained[29].

Besides high ICE and stable cycle life, the fast-charging capability of the anode

materials is also critical in practical applications. Graphite, owing to its low working potential, is not suitable as the anode of fast-charging LIBs. $Li_4Ti_5O_{12}$ can enable ultrafast charging (>10 C), but significantly reduces the energy density of the cell because of its high working potential (~1.5 V vs. Li/Li^+). Si and P are thus more promising anode choices for fast charging, because of their high specific capacity and moderate working voltage, which can reduce the electrode thickness and the charge carrier transport distance as well as avoid Li dendrite formation [30]. Therefore, we further evaluated the cycle stability of the BPC anode under high-rate cycling. As shown in Figure 5a, the BP anode was charged/discharged at 1 C, which can still deliver a high initial reversible capacity of 1968.1 mAh g^{-1} and maintain 1593.2 mAh g^{-1} after 100 cycles, corresponding to a high capacity retention of ~81%. The rate capability of the BPC anode was further evaluated by changing the charge/discharge rate from 0.08 C to 2.4 C, as shown in Figure 5b; the corresponding voltage profiles are shown in Figure 5c. It can be seen that the BPC anode demonstrates excellent rate capability, which showed a specific capacity of 2596, 2511, 2394, 2240, 2178, 2049, 1927 and 1637 mAh g^{-1} at the rate of 0.08 C, 0.16 C, 0.32 C, 0.64 C, 0.8 C, 1.2 C, 1.6 C and 2.4 C, respectively. The result indicated that the lithiation/de-lithiation of the BPC anode is reversible even under fast charging/discharging. The high ICE, excellent cycle and rate capability, and high P loading of the BPC anode make it a clear improvement over other P-based anode materials reported recently. The rate capability of the BPC anode is compared to the previously reported data from P-based anodes for LIBs in Figure 5d. It is obvious that the BPC anode surpasses many other reported P-based anode materials

with similar electrode composition; most of them suffer from significant capacity degradation, with capacities below 1300 mAh g^{-1} at a current density of 4 A g^{-1}, while the BPC anode could still deliver a capacity of over 1600 mAh g^{-1} at 6.25 A g^{-1}.

To further demonstrate the potential practical applications of the BPC anode, full-cell LIBs using the BPC anode and the NCM622 cathode were fabricated. The structure and electrochemical properties of the NCM622 cathode were described in our previous work [31]. In the present work, the negative/positive ratio is controlled at 1.1. As shown in Figure 6a, the BPC/NCM622 full cell demonstrated a high specific charge and discharge capacity of 212.5 and 183.1 mAh g^{-1}, respectively, leading to a high ICE of ~ 86%. Because of the high ICE of the BPC anode, no pre-lithiation is needed to mitigate the irreversible capacity loss. As a result, the BPC/NCM622 full cell demonstrated excellent cycle stability at a current density of 36 mA g^{-1}, maintaining ~ 88% of the initial discharge capacity after 100 cycles (Figure 6b). Moreover, the BPC/NCM622 full cell has an excellent rate capability, as shown in Figures 6c and d. When compared with other anode materials such as graphite and SiO anode, the estimated energy density of NCM622/BPC cell is higher than NCM622/Graphite cell and comparable with NCM622/SiO cell (see Table S1).

Note that the cost of BP is a concern in the practical application of the BPC anode. Thus, we have also fabricated a low-cost red phosphorus/Ketjenblack-MWCNTs (RPC) composite using the same process. As shown in Figure 7a and 7b, despite slightly lower specific capacity than the BPC due to lower electronic conductivity of RP as compared to BP, the RPC anode still demonstrated a high specific capacity of ~ 2000 mAh g^{-1},

stable cycle life, and a high ICE of 87%. Thus, we believe a concept using BP-RP/Ketjenblack-MWCNTs composite would be a practical choice in terms of cost, ICE, specific capacity, cycle life, and rate capability.

Conclusions

In summary, we have fabricated a practical P-based anode material with high initial coulombic efficiency, high reversible capacity, and excellent cycle and rate capability for high-energy lithium-ion batteries through a scalable high-energy ball milling approach. The excellent electrochemical performance can be attributed to the well-accommodated volume changes, suppressed irreversible electrolyte decomposition, and highly reversible phase changes achieved by using the hierarchical micro/nanostructure design concept. This work paves the way to improving the alloying anode materials for high-energy lithium-ion batteries.

Supporting Information

The following is the Supplementary data to this article: Energy density estimation details of lithium-ion batteries using different anode materials.

Declaration of competing interest

The authors declare that they have no known competing financial interests or personal relationships that could have appeared to influence the work reported in this paper.

Acknowledgments

Research at Argonne National Laboratory was funded by the U.S. Department of Energy, Vehicle Technologies Office. Support from Tien Duong of the U.S. DOE's Office of Vehicle Technologies Program is gratefully acknowledged. Use of the

Advanced Photon Source and the Center for Nanoscale Materials, both Office of Science User Facilities, was supported by the U.S. Department of Energy, Office of Science and Office of Basic Energy Sciences, under contract no. DE-AC02-06CH11357.

References

[1] E. Peled, C. Menachem, D. BarTow, A. Melman, Improved graphite anode for lithium-ion batteries-Chemically bonded solid electrolyte interface and nanochannel formation, J. Electrochem. Soc. 143 (1996) L4-L7.

[2] D. Lin, Z. Lu, P.-C. Hsu, H.R. Lee, N. Liu, J. Zhao, H. Wang, C. Liu, Y. Cui, A high tap density secondary silicon particle anode fabricated by scalable mechanical pressing for lithium-ion batteries, Energy Environ Sci. 8 (2015) 2371-2376.

[3] C.-M. Wang, X. Li, Z. Wang, W. Xu, J. Liu, F. Gao, L. Kovarik, J.-G. Zhang, J. Howe, D.J. Burton, Z. Liu, X. Xiao, S. Thevuthasan, D.R. Baer, In Situ TEM Investigation of Congruent Phase Transition and Structural Evolution of Nanostructured Silicon/Carbon Anode for Lithium Ion Batteries, Nano Lett. 12 (2012) 1624-1632.

[4] H. Gao, L.S. Xiao, I. Plume, G.L. Xu, Y. Ren, X.B. Zuo, Y.Z. Liu, C. Schulz, H. Wiggers, K. Amine, Z.H. Chen, Parasitic Reactions in Nanosized Silicon Anodes for Lithium-Ion Batteries, Nano Lett. 17 (2017) 1512-1519.

[5] C.K. Chan, H. Peng, G. Liu, K. McIlwrath, X.F. Zhang, R.A. Huggins, Y. Cui, High-performance lithium battery anodes using silicon nanowires, Nat. Nanotech. 3 (2008) 31-35.

[6] X. Li, M. Gu, S. Hu, R. Kennard, P. Yan, X. Chen, C. Wang, M.J. Sailor, J.G. Zhang, J. Liu, Mesoporous silicon sponge as an anti-pulverization structure for high-performance lithium-ion battery anodes, Nat. Commun. 5 (2014) 4105.

[7] J.-G. Ren, Q.-H. Wu, G. Hong, W.-J. Zhang, H. Wu, K. Amine, J. Yang, S.-T. Lee Silicon–Graphene Composite Anodes for High-Energy Lithium Batteries, Energy Tech. 1 (2013) 77-84.

[8] B. Fuchsbichler, C. Stangl, H. Kren, F. Uhlig, S. Koller, High capacity graphite–silicon composite anode material for lithium-ion batteries, J. Power Sources 196 (2011) 2889-2892.

[9] Y. Jin, S. Li, A. Kushima, X. Zheng, Y. Sun, J. Xie, J. Sun, W. Xue, G. Zhou, J. Wu, F. Shi,

R. Zhang, Z. Zhu, K. So, Y. Cui, J. Li, Self-healing SEI enables full-cell cycling of a silicon-majority anode with a coulombic efficiency exceeding 99.9%, Energy Environ. Sci. 10 (2017) 580-592.

[10] F. Zhang, G. Zhu, K. Wang, X. Qian, Y. Zhao, W. Luo, J. Yang, Boosting the initial coulombic efficiency in silicon anodes through interfacial incorporation of metal nanocrystals, J. Mater. Chem. A, 7 (2019) 17426-17434.

[11] H.C. Jin, H.Y. Wang, Z.K. Qi, D.S. Bin, T.M. Zhang, Y.Y. Wan, J.Y. Chen, C.H. Chuang, Y.R. Lu, T.S. Chan, H.X. Ju, A.M. Cao, W.S. Yan, X.J. Wu, H.X. Ji, L.J. Wan, A Black Phosphorus-Graphite Composite Anode for Li-/Na-/K-Ion Batteries, Angew. Chem. Int. Ed. 59 (2020) 2318-2322.

[12] L. Wang, X.M. He, J.J. Li, W.T. Sun, J. Gao, J.W. Guo, C.Y. Jiang, Nano-Structured Phosphorus Composite as High-Capacity Anode Materials for Lithium Batteries, Angew. Chem. Int. Ed. 51 (2012) 9034-9037.

[13] G.L. Xu, Z.H. Chen, G.M. Zhong, Y.Z. Liu, Y. Yang, T.Y. Ma, Y. Ren, X.B. Zuo, X.H. Wu, X.Y. Zhang, K. Amine, Nanostructured Black Phosphorus/Ketjenblack Multiwalled Carbon Nanotubes Composite as High Performance Anode Material for Sodium-Ion Batteries, Nano Lett. 16 (2016) 3955-3965.

[14] W.Y. Lei, Y.Y. Liu, X.X. Jiao, C.F. Zhang, S.Z. Xiong, B. Li, J.X. Song, Improvement of Cycling Phosphorus-Based Anode with LiF-Rich Solid Electrolyte Interphase for Reversible Lithium Storage, Acs Appl. Energy Mater. 2 (2019) 2699-2707.

[15] J.B. Zhou, X.Y. Liu, W.L. Cai, Y.C. Zhu, J.W. Liang, K.L. Zhang, Y. Lan, Z.H. Jiang, G.M. Wang, Y.T. Qian, Wet-Chemical Synthesis of Hollow Red-Phosphorus Nanospheres with Porous Shells as Anodes for High-Performance Lithium-Ion and Sodium-Ion Batteries, Adv. Mater. 29 (2017) 1700214.

[16] Y. Yang, X. Liu, Z. Dai, F. Yuan, Y. Bando, D. Golberg, X. Wang, In Situ Electrochemistry of Rechargeable Battery Materials: Status Report and Perspectives, Adv. Mater. 29 (2017) 1606922.

[17] X.X. Jiao, Y.Y. Liu, T.T. Li, C.F. Zhang, X.Y. Xu, O.O. Kapitanova, C. He, B. Li, S.Z. Xiong, J.X. Song, Crumpled Nitrogen-Doped Graphene-Wrapped Phosphorus Composite as a Promising Anode for Lithium-Ion Batteries, Acs Appl. Mater. Interfaces 11 (2019) 30858-

30864.

[18] Z.X. Yu, J.X. Song, M.L. Gordin, R. Yi, D.H. Tang, D.H. Wang, Phosphorus-Graphene Nanosheet Hybrids as Lithium-Ion Anode with Exceptional High-Temperature Cycling Stability, Adv. Sci. 2 (2015) 1400020.

[19] Z.S. Yue, T. Gupta, F. Wang, C. Li, R. Kumar, Z.Y. Yang, N. Koratkar, Utilizing a graphene matrix to overcome the intrinsic limitations of red phosphorus as an anode material in lithium-ion batteries, Carbon 127 (2018) 588-595.

[20] L. Sun, Y. Zhang, D.Y. Zhang, Y.H. Zhang, Amorphous red phosphorus nanosheets anchored on graphene layers as high performance anodes for lithium ion batteries, Nanoscale 9 (2017) 18552-18560.

[21] Y.P. Zhang, L.L. Wang, H. Xu, J.M. Cao, D. Chen, W. Han, 3D Chemical Cross-Linking Structure of Black Phosphorus@CNTs Hybrid as a Promising Anode Material for Lithium Ion Batteries, Adv. Funct. Mater. (2020) 1909372.

[22] X.X. Jiao, Y.Y. Liu, B. Li, W.X. Zhang, C. He, C.F. Zhang, Z.X. Yu, T.Y. Gao, J.X. Song, Amorphous phosphorus-carbon nanotube hybrid anode with ultralong cycle life and high-rate capability for lithium-ion batteries, Carbon 148 (2019) 518-524.

[23] T. Yuan, J.F. Ruan, C.X. Peng, H. Sun, Y.P. Pang, J.H. Yang, Z.F. Ma, S.Y. Zheng, 3D red phosphorus/sheared CNT sponge for high performance lithium-ion battery anodes, Energy Storage Mater. 13 (2018) 267-273.

[24] Y. Sun, L. Wang, Y. Li, Y. Li, H.R. Lee, A. Pei, X. He, Y. Cui, Design of Red Phosphorus Nanostructured Electrode for Fast-Charging Lithium-Ion Batteries with High Energy Density, Joule 3 (2019) 1080-1093.

[25] W.C. Chang, K.W. Tseng, H.Y. Tuan, Solution Synthesis of Iodine-Doped Red Phosphorus Nanoparticles for Lithium-Ion Battery Anodes, Nano Lett. 17 (2017) 1240-1247.

[26] H. Liu, S.X. Zhang, Q.Z. Zhu, B. Cao, P. Zhang, N. Sun, B. Xu, F. Wu, R.J. Chen, Fluffy carbon-coated red phosphorus as a highly stable and high-rate anode for lithium-ion batteries, J. Mater. Chem. A 7 (2019) 11205-11213.

[27] X. Zhou, T. Li, Y. Cui, Y. Fu, Y. Liu, L. Zhu, In Situ Focused Ion Beam Scanning Electron Microscope Study of Microstructural Evolution of Single Tin Particle Anode for Li-Ion Batteries, Acs Appl. Mater. Interfaces 11 (2019) 1733-1738.

[28] B.Q. Xiong, X.W. Zhou, G.L. Xu, Y.Z. Liu, L.K. Zhu, Y.C. Hu, S.Y. Shen, Y.H. Hong, S.C. Wan, X.C. Liu, X. Liu, S.L. Chen, L. Huang, S.G. Sun, K. Amine, F.S. Ke, Boosting Superior Lithium Storage Performance of Alloy-Based Anode Materials via Ultraconformal Sb Coating-Derived Favorable Solid-Electrolyte Interphase, Adv. Energy Mater. 10 (2020) 1903186.

[29] J.X. Song, Z.X. Yu, M.L. Gordin, S. Hu, R. Yi, D.H. Tang, T. Walter, M. Regula, D. Choi, X.L. Li, A. Maniyannan, D.H. Wang, Chemically Bonded Phosphorus/Graphene Hybrid as a High Performance Anode for Sodium-Ion Batteries, Nano Lett. 14 (2014) 6329-6335.

[30] Y. Liu, Y. Zhu, Y. Cui, Challenges and opportunities towards fast-charging battery materials, Nat. Energy 4 (2019) 540-550.

[31] X.Q. Zeng, G.L. Xu, Y. Li, X.Y. Luo, F. Maglia, C. Bauer, S.F. Lux, O. Paschos, S.J. Kim, P. Lamp, J. Lu, K. Amine, Z.H. Chen, Kinetic Study of Parasitic Reactions in Lithium-Ion Batteries: A Case Study on $LiNi_{0.6}Mn_{0.2}Co_{0.2}O_2$, Acs Appl. Mater. Interfaces 8 (2016) 3446-3451.

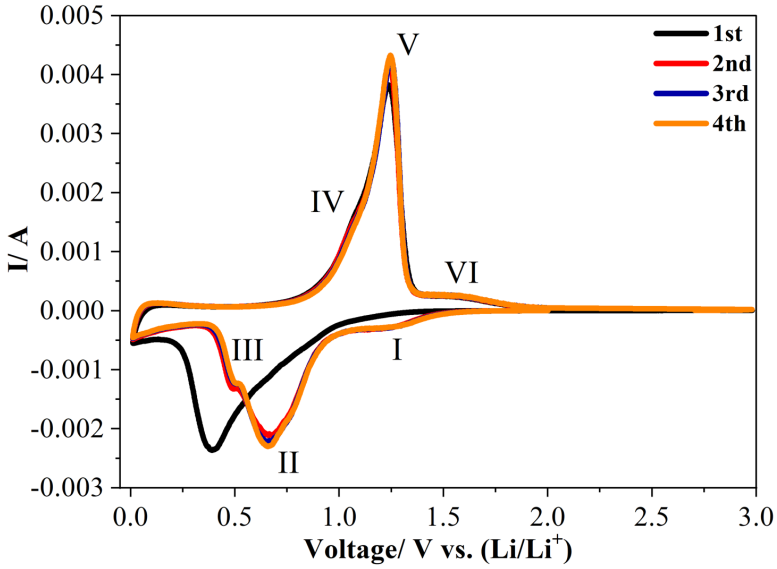

Figure 1 The first four cyclic voltammograms of the BPC anode at a scan rate of 0.1 mV s^{-1}.

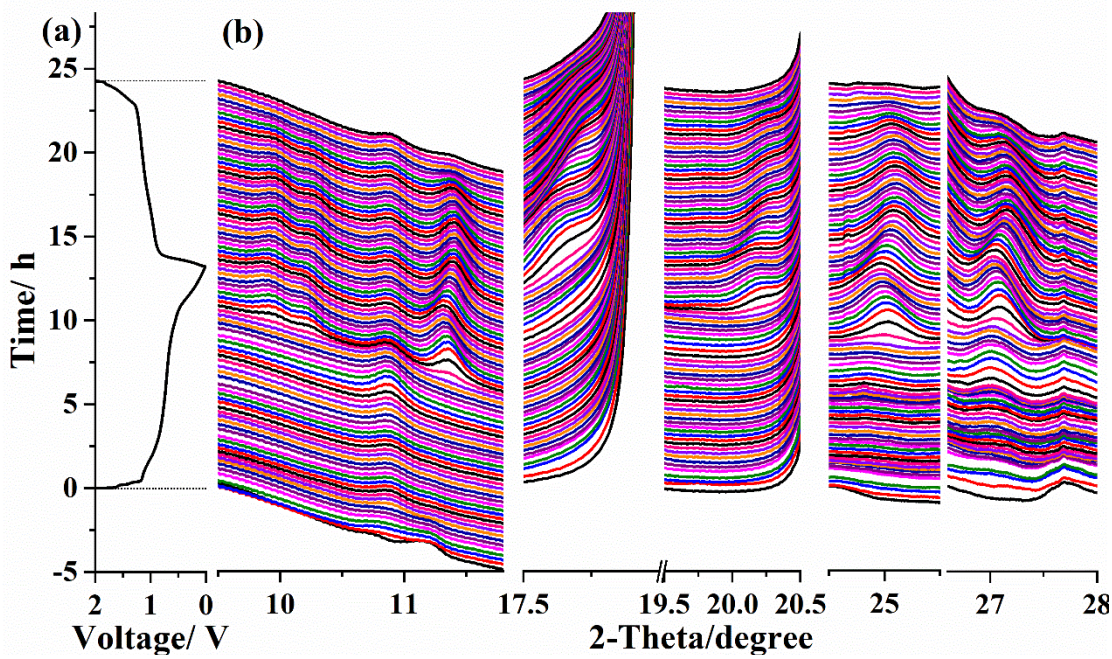

Figure 2 (a) The voltage profile of the BPC anode at 0.1 C and (b) the corresponding HEXRD patterns during charge/discharge.

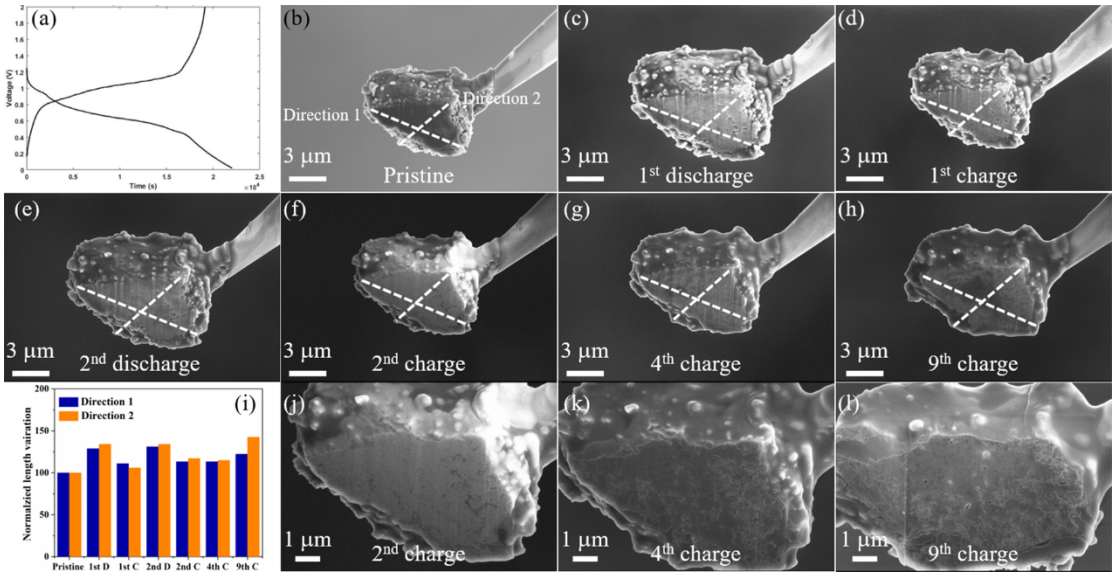

Figure 3 (a) The initial lithiation/de-lithiation curves and (b-h) the corresponding in situ SEM images of a single BPC particle. (i) Normalized length variation of the BPC particle in different stages of charge/discharge and cycles. We defined the length as 100% in two directions in the pristine state. (j-l) Cross-sectional SEM image of the BPC particle at different cycles.

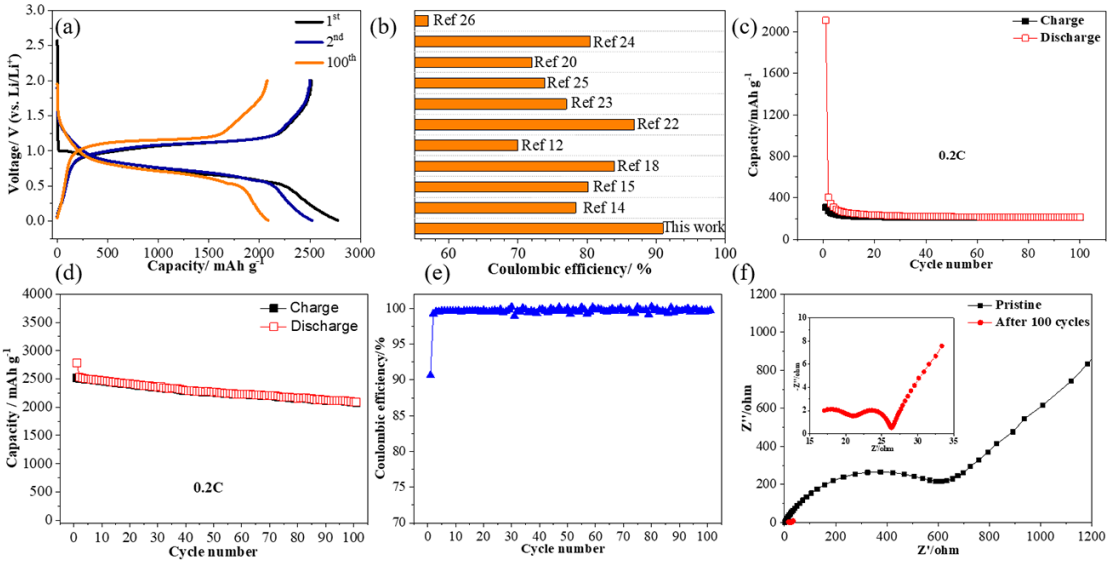

Figure 4 (a) Charge/discharge profiles of the BPC anode at 0.2 C. (b) Comparison of the initial coulombic efficiency of the BPC anode with other reported P-based anodes. Cycle performance of (c) the Ketjenblack/MWCNTs electrode and (d) the BPC anode at 0.2 C. (e) Coulombic efficiency of the BPC anode during cycling at 0.2 C. (f) Electrochemical impedance spectroscopy of the Li/BPC anode before and after 100 cycles of charge/discharge at 0.2 C.

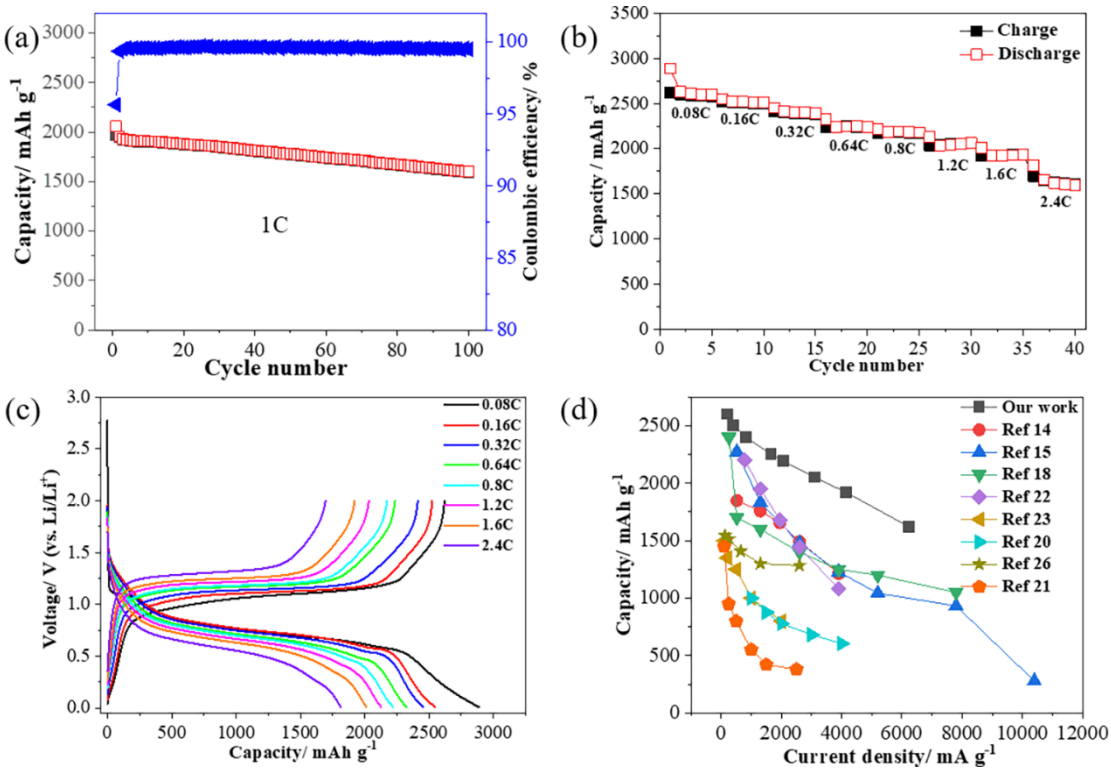

Figure 5 (a) Cycle performance of the BPC anode at 1 C. (b) Rate capability and (c) voltage profiles of the BPC anode at different charge/discharge rates. (d) Comparison of the rate capability of the BPC anode with other reported P-based anodes.

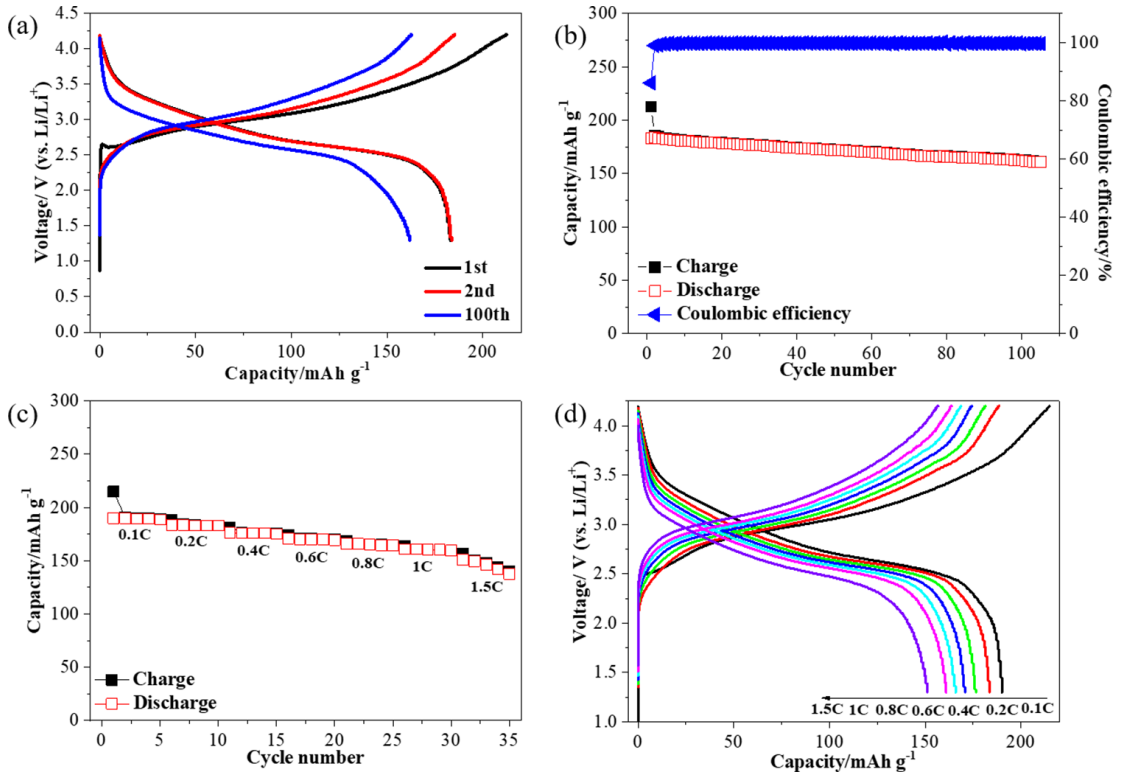

Figure 6 (a) Representative charge/discharge curves, (b) cycle performance at 36 mA g^{-1}, and (c, d) rate performance of the BPC/$LiNi_{0.6}Co_{0.2}Mn_{0.2}O_2$ full cell.

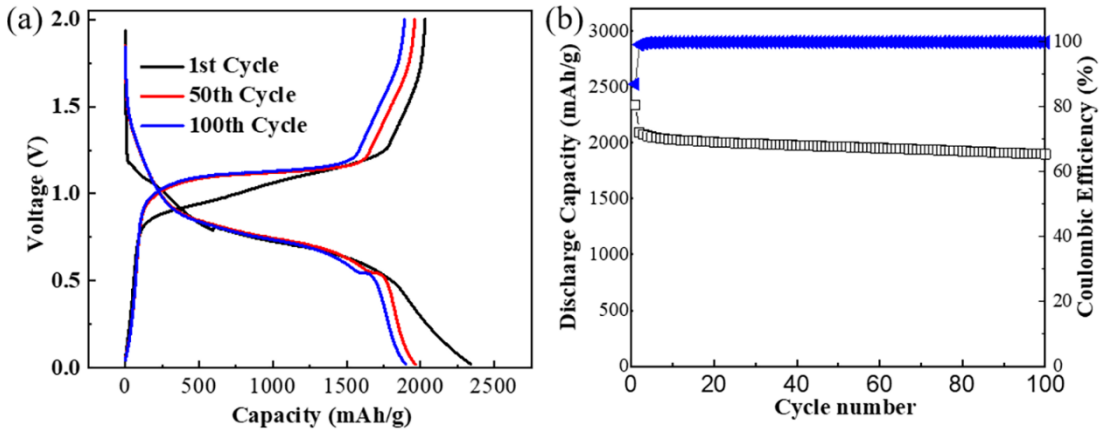

Figure 7 (a) Charge/discharge profiles and (b) cycle performance of the RPC anode at 0.2 C.

Authors biography

Rachid Amine is currently an assistant chemist at Argonne National Laboratory since 2013. His research efforts have focused on the development of high energy materials and beyond lithium ion technologies.

Daali Amine is currently a PhD candidate at University of Wisconsin-Milwaukee. He is also a Co-op student at Argonne National Laboratory. His research focus on the development of high capacity electrode materials for room temperature sodium-ion batteries.

Xinwei Zhou received his B.S. degree from department of mechanical engineering, Zhejiang University in 2012. He received his M.S. degree from department of mechanical engineering, New Jersey Institute of Technology in 2015. He is now a PhD candidate under the supervision of Prof. Likun Zhu at Purdue University. He is also a graduate visiting student at Center of Nanoscale Materials of Argonne National Laboratory. His research focus on lithium-ion batteries and in situ electron microscopy studies.

Dr. Xiang Liu is now work as postdoctoral researcher at Argonne National Laboratory. He obtained his PhD from the University of Hong Kong in 2016. Prior to his current position, he worked as a postdoc in Automotive Department in Tsinghua University. His research focus includes cathode material design and synthesis for lithium-ion and sodium-ion batteries, as well as the in situ/operando synchrotron X-ray based characterizations for the understanding of battery safety and degradation mechanisms.

Dr. Yuzi Liu is an assistant scientist in the Center for Nanoscale Materials (CNM) at Argonne National Laboratory. He received his Ph.D. degree in condensed matter physics from Institute of Physics, Chinese Academy of Sciences in 2007. He then worked as a postdoc in University of Texas at Arlington and a visiting scholar at Georgia Institute of Technology in Prof. ZL Wang's group and Ames Lab. Then, he moved to Materials Science Division at ANL as a division postdoc appointee. In 2011, he joined CNM at ANL working on microstructure characterization by in situ and ex situ TEM on energy materials.

Dr. Yang Ren received his M.S. degree in condensed matter physics from the Institute of Physics, Chinese Academy of Science, China, and his Ph.D. degree in Chemical Physics from the University of Groningen, The Netherlands. He is currently a physicist and lead beamline scientist at the Advanced Photon Source, Argonne National Laboratory, USA. His research interests focus on the structure-property studies of materials by utilizing synchrotron X-ray and neutron scattering and other techniques. His research activities include the investigation of phase transition, correlated electron systems, engineering materials, nanoparticles and nanocomposites, energy storage and conversion materials.

Dr. Xiaoyi Zhang received her Ph.D. in chemical physics from the University of Maryland at College Park in 2003, under the supervision of Prof. Robert A. In 2005, she moved to Argonne National Laboratory as a postdoctoral fellow. In 2007, she became an Assistant Physicist at Argonne and promoted to Physicist in 2012. Xiaoyi Zhang's research focuses on understanding the ultrafast dynamics and structural-functional correlations of solar energy materials using various time-resolved X-ray techniques combined with ultrafast laser spectroscopy. She is the lead developer of the time-resolved X-ray absorption spectroscopy and diffraction techniques at beamline 11-ID-D.

Dr. Likun Zhu is an associate professor in the Department of Mechanical and Energy Engineering at Indiana University Purdue University Indianapolis. He received his PhD degree from the University of Maryland in 2006. He serves as an Editorial Advisory Board member for Energy & Environmental Materials. His main research interests are advanced materials for lithium ion batteries, in situ and operando characterization techniques, modeling, simulation and optimization of battery systems, and micro/nano fabrication.

Dr. Said Al-Hallaj is the CEO and co-founder of All Cell Technologies LLC, and a Research Professor of Chemical Engineering at The University of Illinois at Chicago. He earned his B.Sc and M.Sc in Chemical Engineering from Jordan University of Science and Technology and a Ph.D. in Chemical Engineering from the Illinois Institute of Technology. He co-authored a book entitled "Hybrid Hydrogen Systems" and has published several book chapters and numerous numbers of peer-reviewed and conference journal papers. Said is the co-inventor of several issued and pending patent applications in the areas of renewable energy, energy storage and water desalination.

Dr. Zonghai Chen obtained his PhD from Dalhousie University of Canada (2004), and currently is a chemist at Argonne National Laboratory. His research interest includes functional electrolytes, electrode materials and in situ techniques for advanced lithium ion batteries. Dr. Chen has authors/co-authored more than 120 peer-reviewed research articles and has a dozen of U.S. patent and patent application.

Dr. Gui-Liang Xu is currently an assistant chemist in the Electrochemical Energy Storage group under the division of Chemical Sciences and Engineering at Argonne National Laboratory. His researches focus on both fundamental understanding and materials development for lithium-ion batteries and beyond. Dr. Xu earned his Bachelor (2009) and PhD (2014) degree in the department of Chemistry of Xiamen University. After three years postdoc research at Argonne, he was promoted to permanent staff scientist. Dr. Xu has authors/co-authored over 70 peer-reviewed research articles and has 2 granted U.S. patent and several patent applications.

Dr. Khalil Amine is Argonne Distinguished Fellow and the leader of the Advanced Battery Technology team at Argonne National Laboratory, where he is responsible for directing the research and development of advanced materials and battery systems for HEV, PHEV, EV, and satellite applications. He is an adjunct professor at Stanford University. Among his many awards, Dr. Amine is the 2019 reception of the prestigious Global Energy Prize. He is a six-time recipient of the R&D 100 Award, which is considered as the Oscar of technology and innovation. He is an ECS fellow, and associate editor of the journal of Nano-Energy.